MECHANISMS OF DEVELOPMENT 129 (2012) 244–254

Available at www.sciencedirect.com
SciVerse ScienceDirect
journal homepage: www.elsevier.com/locate/modo

Rgs19 regulates mouse palatal fusion by modulating cell proliferation and apoptosis in the MEE

Wern-Joo Sohn [a,b,1], *Young-Rae Ji* [a,1], *Hyeng-Soo Kim* [a], *Gi-Jeong Gwon* [b], *Young-Mi Chae* [b], *Chang-Hyeon An* [c], *Hyun-do Park* [d], *Han-Sung Jung* [e], *Zae Young Ryoo* [a], *Sanggyu Lee* [a], *Jae-Young Kim* [b,*]

[a] *School of Life Science and Biotechnology, Kyungpook National University, Daegu, Republic of Korea*
[b] *Department of Biochemistry, School of Dentistry, IHBR, Kyungpook National University, Daegu, Republic of Korea*
[c] *Department of Oral and Maxillofacial Radiology, School of Dentistry, IHBR, Kyungpook National University, Daegu, Republic of Korea*
[d] *Forensic Science, Busan Metropolitan Police Agency, Busan, Republic of Korea*
[e] *Division in Anatomy and Developmental Biology, Department of Oral Biology, Research Center for Orofacial Hard Tissue Regeneration, Brain Korea 21 Project, Oral Science Research Center, College of Dentistry, Yonsei Center of Biotechnology, Yonsei University, Seoul, Republic of Korea*

ARTICLE INFO

Article history:
Received 31 January 2012
Received in revised form
18 July 2012
Accepted 18 July 2012
Available online 27 July 2012

Keywords:
Palatogenesis
Rgs19
Apoptosis
Genome wide screening
Palatal fusion

ABSTRACT

Palatal development is one of the critical events in craniofacial morphogenesis. During fusion of the palatal shelves, removal of the midline epithelial seam (MES) is a fundamental process for achieving proper morphogenesis of the palate. The reported mechanisms for removing the MES are the processes of apoptosis, migration or general epithelial-to-mesenchymal transition (EMT) through modulations of various signaling molecules including Wnt signaling. RGS19, a regulator of the G protein signaling (RGS) family, interacts selectively with the specific α subunits of the G proteins (Gαi, Gαq) and enhances their GTPase activity. Rgs19 was reported to be a modulator of the Wnt signaling pathway. In mouse palatogenesis, the restricted epithelial expression pattern of Rgs19 was examined in the palatal shelves, where expression of Wnt11 was observed. Based on these specific expression patterns of Rgs19 in the palatal shelves, the present study examined the detailed developmental function of Rgs19 using AS-ODN treatments during *in vitro* palate organ cultivations as a loss-of-function study. After the knockdown of Rgs19, the morphological changes in the palatal shelves was examined carefully using a computer-aided three dimensional reconstruction method and the altered expression patterns of related signaling molecules were evaluated using genome wide screening methods. RT-qPCR and *in situ* hybridization methods were also used to confirm these array results. These morphological and molecular examinations suggested that Rgs19 plays important roles in palatal fusion through the degradation of MES via activation of the palatal fusion related and apoptotic related genes. Overall, inhibition of the proliferation related and Wnt responsive genes by Rgs19 are required for proper palatal fusion.

* Corresponding author. Address: Kyungpook National University, 101 Dongin-dong 2ga, Joong-gu, Daegu 700-422, Republic of Korea. Tel.: +82 53 420 4998; fax: +82 53 421 4276.
E-mail address: jykim91@knu.ac.kr (J.-Y. Kim).

Abbreviations: MEE, medial edge epithelium; MES, midline epithelial seam; EMT, epithelial-to-mesenchymal transition.

[1] First two authors contributed equally to this work.

0925-4773/$ - see front matter
http://dx.doi.org/10.1016/j.mod.2012.07.004

1. Introduction

The palatal shelves originate bilaterally from the internal surface of the maxillary prominence. They are positioned and grow vertically on each side of the tongue. After growth, the subsequent palatal shelves elevate and fuse to a horizontal position above the tongue. They are fused with one another from the middle region to the adjacent regions, and the medial edge epithelia (MEE) then transforms to the midline epithelial seam (MES) (Chou et al., 2004; Martinez-Alvarez et al., 2000). The failure of these harmonized procedures can result in birth defects, such as a cleft lip and palate (Gritli-Linde, 2007; Lee et al., 2008; Liu et al., 2005; Taniguchi et al., 1995; Yu et al., 2009).

A cleft palate is a defect of craniofacial development and results from a dysfunction of palatal growth, shelf elevation and a MEE disappearance between the two secondary palatal shelves (Kang and Svoboda, 2002). The fate of the MEE, which forms the MES after palatal shelf fusion, is unclear. The three main mechanisms that account for the loss of MEE would be apoptosis (Cuervo and Covarrubias, 2004), epithelial migration (Jin and Ding, 2006) and an epithelial-to-mesenchymal transition (EMT) (Nawshad, 2008; Nawshad and Hay, 2003). Previously, the interactions between Wnt11 and Fgfr1b, which are key factors in convergent extension, modulate palatal cell proliferation for growth and apoptosis to fuse the palatal shelves (Kemler et al., 2004; Lee et al., 2008; Logan et al., 1999 In addition to these epithelial-mesenchymal interactions, several significant signaling pathways including TGFβ, BMP, FGF and Notch would involve in palatogenesis (Gritli-Linde, 2007; Lee et al., 2008; Liu et al., 2005; Taniguchi et al., 1995; Yu et al., 2009). In particular, during palate fusion, TGFβ3, Snail and Lef1 were established as essential growth and transcription factors inducing the removal of MES during palatal fusion (Nawshad, 2008; Nawshad and Hay, 2003). The Wnt family of secreted cytokines have been reported to be functionally important signaling molecules during palatogenesis (Chiquet et al., 2008; He et al., 2008; Lee et al., 2008; Warner et al., 2009). In many developmental processes, such as gastrulation and ectodermal formation of blastocysts, EMT is induced by the Wnt/β-catenin signaling pathways (Kemler et al., 2004; Logan et al., 1999).

The regulator of the G protein signaling (RGS) family consist of more than 20 members (De Vries et al., 2000). The RGS proteins play the role of GTPase and interact with the GTP-Gα subunits to limit their lifespan and terminate the downstream signaling pathways (Hollinger and Hepler, 2002; Ross and Wilkie, 2000). RGS19 is one of the first RGS members discovered and interacts selectively with the specific α subunits of the G proteins (Gαi, Gαq) and enhances their GTPase activity (De Vries et al., 1995). In addition, Rgs19 was examined as a regulator that attenuates Wnt signaling via inactivation of the Gαo subunit (Feigin and Malbon, 2007). In addition, a recent report showed that Rgs19 affects cardiac development and has negative effects on the heart function (Ji et al., 2010). Restricted Rgs19 expression was detected in the MEE of the palatal shelves in which Tgfβ3 and Wnt11 were expressed (Yang et al., 2008; Lee et al., 2008).

After knocking down of Rgs19, the morphological changes in palatal fusion and the altered expression patterns of the signaling molecules were examined using a genome wide screening method. The expression patterns of the candidate genes were then confirmed by RT-qPCR and *in situ* hybridization. In addition, the altered cellular events, such as cell proliferation and apoptosis, were evaluated to define the presumptive roles and signaling pathways of Rgs19 in palatogenesis.

2. Materials and methods

All experiments were performed according to the guidelines of the Kyungpook National University, School of Dentistry, Intramural Animal Use and Care Committee.

2.1. Animals

Adult ICR mice were housed in a temperature-controlled room (22 °C) under artificial illumination (lights on from 05:00 to 17:00), at 55% relative humidity, with free access to food and water. Mouse embryos were obtained from time-mated pregnant mice. The day on which a vaginal plug was confirmed then designated as embryonic day 0 (E0). We collected the time-designated embryos based on the morphological criteria, provided from the "the mouse atlas project" (http://www.emouseatlas.org).

2.2. In vitro organ culture

Procedures for *in vitro* organ culture were carried out at E13 for 1 or 2 days as described previously (Sohn et al., 2011). After the removal of brain forming tissues, dissected maxilla region including palatal shelves were cultivated in a 8-ml of BGJb medium containing 1% penicillin–streptomycin for 1 or 2 days in a 50-ml penicillin bottle. Three or four explants were put into one bottle, and the bottle was sealed airtightly using a rubber stopper and a metal clamp. The bottles were flushed for approximately 2 min with a gas mixture of 50% O_2, 45% N_2, and 5% CO_2. The bottles were incubated at 37 °C on a roller device (20 rpm) for 1 or 2 days. The culture bottles were flushed every 24 h with the same gas mixture. For Trowell's modified cultivations, palatal shelves were isolated from E13 mouse maxillae and cultured in medium without fetal bovine serum at 37 °C and 5% CO_2 for 1 or 2 days (Lee et al., 2008). The culture medium (DMEM/F12, Gibco) was supplemented with 20 μg/ml ascorbic acid (Sigma) and 1% penicillin/streptomycin and was renewed every 24 h.

2.3. Antisense-oligodeoxynucleotide (AS-ODN) treatments

AS-ODNs for Rgs19 were designed and treated during *in vitro* rolling organ culture (Hoffman et al., 2002; Kim et al., 2005; Mailleux et al., 2001). ODNs were designed as AS-ODN Rgs19 5′-TGTTTCTCAGCCTCATGT-3′, Sense (S)-ODN 5′-ACATGAGGCTGAGAAACA-3′. FITC-tagged Rgs19 AS-ODNs were used to detect the penetration level of AS-ODNs into the palate tissue. These ODNs were purchased from GENOTECH

(Korea). The optimal Rgs19 AS-ODN concentration was determined based on the morphology of the cultured explants after tests at various concentrations (5 nM–30 μM). They were added into the culture medium at a final concentration of 2 μM.

2.4. RNA extraction and real time quantitative PCR

Total RNA was isolated from the specimens, collected and pooled from the at least 10 specimens, using the RNeasy Micro Kit (Qiagen, USA). For cDNA synthesis, reverse transcription was performed using RT-PCR kit (Takara, Japan). Real time quantitative PCR (RT-qPCR) was performed using ABI 7300 Real Time PCR System (Applied Biosystems, USA) with SYBR Green PCR master mix (Applied Biosystems, USA). The results of RT-qPCR for each sample were normalized by GAPDH. The results were expressed as normalized ratios. The primer sequences of the genes are presented in the Fig. 5. Data were expressed as mean ± SD. The mean expression levels were compared between the experimental and control groups using student *t*-test.

2.5. Sample selection and Mouse Gene 1.0 ST array

After the one day cultivation at E13, S-ODN and AS-ODN treated specimens were collected and prepared respectively. For each experiment, at least 10 specimens were used respectively. RNA that had high RNA integrity Number (RIN > 9.0; RIN, developed by Agilent Technologies) and had A260/A280 absorbance ratio ranging from 1.8 to 2.1 was used for cDNA synthesis. Gene expression profiles were analyzed on GeneChip® Mouse Gene 1.0 ST array (Affymetrix, Santa Clara, CA) containing 28,853 gene-level probe sets. The Mouse Gene 1.0 ST array interrogates 28,853 well-annotated genes with 770,317 distinct probes. The design of the array was based on the February 2006 mouse genome sequence (UCSC mm8, NCBI build 36) with comprehensive coverage of RefSeq, putative complete CDS GeneBank transcripts, all Ensembl transcript classes and synthetically mapped full-length mRNAs and RefSeq NMs from human and rat. The Mouse Gene 1.0 ST Array has 100 percent coverage of NM sequences present in the April 3, 2007, Ref Seq database. The stained GeneChip probe array was scanned with a GeneChip® Scanner 3000 (Affymetrix) 7G a 570 nm. The signal intensity of the gene expression level was calculated by Expression Console™ software, Version 1.1 (Affymetrix).

2.6. Histology and Immunohistochemistry

Sections were routinely stained with hematoxylin and eosin (H-E) and evaluated by light microscopy. Specimens were fixed in 4% paraformaldehyde (PFA) in phosphate-buffered saline (PBS) overnight at 4 °C, embedded in paraffin wax using conventional methods and then cut to a thickness of 7 μm. Primary antibodies were used to Ki67 (Neo Markers, USA; cat. No. RM-9106), pan-Cytokeratins (Thermo scientific, USA; cat. No. MS-343). Secondary antibodies were used biotinylated goat anti-rabbit or anti-mouse IgG. The binding of primary antibody to the sections was visualized by using a diaminobenzidine tetrahydrochloride (DAB) reagent kit (Zymed, USA; cat. No. 00-2014).

2.7. TUNEL assay

A TUNEL assay was performed using an *in situ* cell apoptosis detection kit (Trevigen, USA) following the manufacturer's instructions. The 7-μm-thick sections were treated with proteinase K [in 10 mM Tris–HCl (pH 8.0)] at a concentration of 20 μg/μl for 15 ∼ 20 min at room temperature. The samples were then incubated with the labeling reaction mixture at 37 °C for 1 h and streptavidin–HRP solution for 10 min at room temperature. DAB was used as a substrate solution to detect the sites of *in situ* apoptosis under a light microscope. At least 10 specimens were examined in each experiment.

2.8. Three-dimensional reconstruction

All the stained sections were photographed using a DM2500 microscope (Leica, Germany). MES regions were reconstructed for each specimen. 'Reconstruct' software was used to reconstruct the 3D images. Serial frontal sections with 5 μm thickness along with the upper molar regions were reconstructed. The images were aligned both automatically and manually using the software. Measurement of area was used by Image J software.

2.9. In situ hybridizations

Whole mount *in situ* hybridization on whole mouse embryos was performed as previously described (Kim et al., 2009) and section *in situ* hybridization was performed as a previously described on wax section by using standard protocols (Kim et al., 2005). Digoxigenin (DIG)-labeled RNA probes were pre-warmed to 80 °C and hybridized overnight at 65 °C. Mouse Rgs19 open reading frame (ORF) plasmids were used with designed primer by GenBank NM_026446.3. Antisense probe was synthesized by SP6 RNA polymerase and used as templates for the synthesis of DIG-labeled RNA probes. After the whole mount *in situ* hybridizations, 20 μm frontal frozen sections were prepared to examine the detailed expression pattern of Rgs19.

2.10. Statistical analysis

All experiments were performed a minimum of three times. Two-sample *t*-tests (equal variance) were used to analyze the significance of difference. $P < 0.05$ was considered statistically significant. For evaluations of Ki67 and TUNEL positive cells, at least 30 palate organ cultures were used in each experiment.

3. Results

3.1. Expression pattern of Rgs19 in palatal development

Detailed gene expression patterns were examined to define the developmental function of *Rgs19* in palate development using whole mount *in situ* hybridization methods.

From E12 to E14, a specific epithelial expression pattern of *Rgs19* was observed in the palatal shelves (Fig. 1). At E12, *Rgs19* was expressed broadly along the palatal shelves (Fig. 1A). The frontal sections showed the epithelial restricted expression pattern of *Rgs19* (Fig. 1B and C). At E13, *Rgs19* was expressed with high intensity in the medial edge epithelial (MEE) region of the palatal shelves (Fig. 1D–F). At E13.5, the palatal shelves were elevated above the tongue before contacting each other, and much stronger and restricted expression pattern of Rgs19 was detected in the MEE region of the palatal shelves (Fig. 1G–I). After palatal fusion, at E14, the epithelial expression pattern of Rgs19 decreased in the MEE (Fig. 1J–L). In particular, *Rgs19* expression was observed mainly in the entire palatal fusion regions, with the exception of the midline epithelial seam (MES) region. This specific expression pattern was similar to that of Wnt11 (Lee et al., 2008). On the other hand, at E14, the posterior palatal shelves showed the remaining epithelial expression pattern of *Rgs19* in the MEE region, which is similar to those of the middle part of the palatal shelves at E13.5 (Fig. 1M and N). Section *in situ* hybridization was also examined at E14 and E14.5 to determine if the epithelial expression of Rgs19 is the result of penetration problems of the mRNA probes. As observed after whole mount *in situ* hybridization, Rgs19 was only expressed in the MEE region at E14, and there was no Rgs19 expression either in the epithelium and mesenchyme of the fused palate at E14.5 (data not shown).

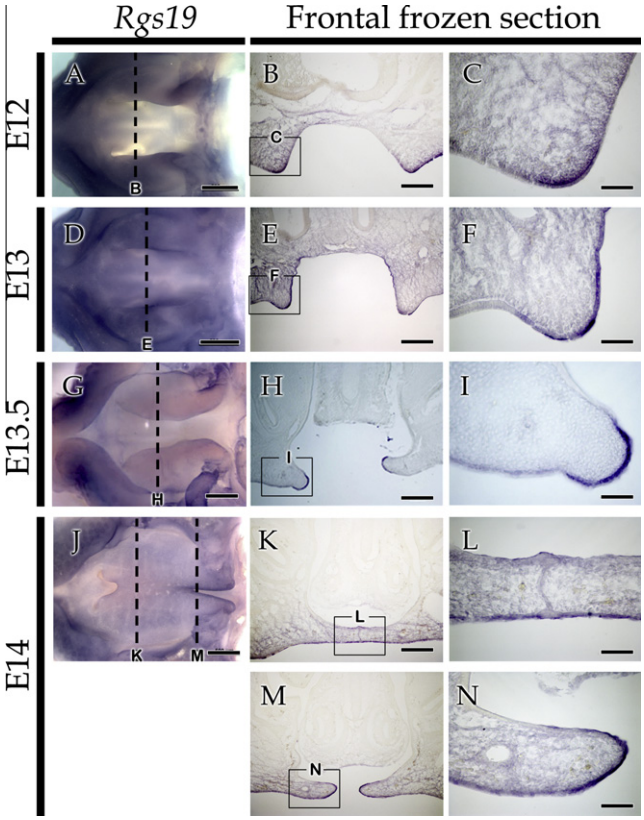

Fig. 1 – Expression pattern of Rgs19 during mice palatogenesis. Rgs19 expression pattern is detected by whole mount *in situ* hybridization and frontal frozen sectioning. (A–C) At E12, epithelial expression of Rgs19 is examined in the edge of the palatal shelf. (D–F) At E13, restricted epithelial expression of Rgs19 is observed along the MEE region. (G–I) At E13.5, Rgs19 is expressed in the MEE region in the elevated palatal shelves. (J–L) At E14, weak and broad expression pattern of Rgs19 is examined in the contacting palatal shelves of the middle part of palate. (J, M and N) posterior parts of palates still shows similar expression pattern to those of E13.5. Black dotted lines indicate the section level; scale bars: A, D, G, J, 500 μm; B, E, H, K, M, 200 μm; C, F, I, L, N, 50 μm.

3.2. *Evaluation of Rgs19 AS-ODN treatments using in vitro organ culture*

This specific epithelial expression pattern of *Rgs19* in the palatal fusion region suggests that Rgs19 plays an important role in mouse palatal fusion. In this study, the AS-ODN (antisense-oligodeoxynucleotide) method was used during the *in vitro* palatal organ cultures at E13 for 1 or 2 days as a loss-of-function study to determine the precise developmental function of Rgs19 in palatogenesis. This *in vitro* organ culture system could mimic the *in vivo* palatal development properly (Fig. 2A, C and E). At E13, the 1 day cultivated specimens showed similar morphological changes to those of the E14 palate with palatal fusion (Fig. 2A; fused palates of control 28/30; 93.3% and S-ODN 12/15; 80%). Compared to the control cultured specimens, AS-ODN for the Rgs19-treated specimens showed defects in palatal fusion (Fig. 2B; fused palates 11/30; 36.7%). After 2 days cultivations at E13, the S-ODN and AS-ODN treated specimens showed similar results to palatal fusion (data not shown). On the other hand, the histological examinations revealed significant differences in the remaining MES between them. None of the S-ODN treated specimens showed MES remaining (14/14; 100%) but 78.6% of the AS-ODN treated specimens (11/14; 78.6%) showed residual MES. A 1 day *in vitro* organ culture was treated with FITC-modified AS-ODN at E13 to evaluate the penetration of AS-ODN for Rgs19 during the *in vitro* organ culture (Fig. 2B, D and F). FITC-modified AS-ODNs were detected in the 24 h cultivated palatal shelves under fluorescent microscopy, whereas the FITC-modified S-ODNs were not detected in control cultured specimens (Fig. 2C–F). The decreased expression pattern of *Rgs19* was confirmed by *in situ* hybridization and RT-qPCR (Figs. 2G, H and J). After selecting the unfused specimens, the palatal shelves were dissected carefully excluding the upper molar tooth germ, and the expression patterns of *Rgs19* from the both control and AS-ODN treated specimens were examined (Fig. 2I). After palatal fusion, Rgs19 expression disappeared. The *in situ* hybridization experiments showed a lower expression pattern of epithelial *Rgs19* in the AS-ODN treated specimen compared to the control cultured specimens (Figs. 2G, H). In addition, the knockdown of *Rgs19* by the AS-ODN treatment showed an almost 50% decrease in the levels of expression compared to those of the control and S-ODN treatment (Fig. 2J). The efficiency and penetration rate of AS-ODN for the knockdown of Rgs19 were examined using the obvious down-regulation of *Rgs19* mRNA expression.

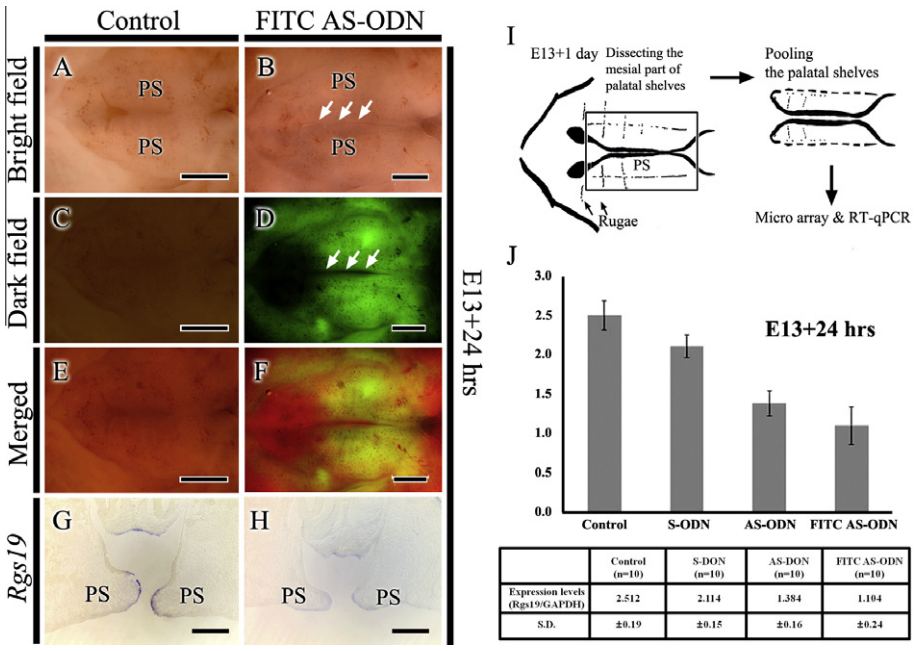

Fig. 2 – Loss-of-function study of Rgs19 by AS-ODN treatments at E13 for 24 h cultivation. (A, C, E and G) Control specimen shows similar developmental processes with Rgs19 expression in the MEE region to those of E14 after 24 h cultivations at E13. (E) Merged figure of A and C. (B) AS-ODN treated specimen shows the retardation of palatal fusion. (D) FITC modified AS-ODN is examined under the fluorescent microscope. (F) Merged figure of B and D. (B and D) White arrows indicate the failure of palatal fusion. (H) Expression pattern of Rgs19 is decreased after the AS-ODN treatment. (I) Schematic diagram for collecting and pooled palatal shelves for RT-qPCR and microarray. (J) Efficiency of AS-ODN for Rgs19 is examined by examination of expression levels of Rgs19 by RT-qPCR. Rgs19 expression levels decrease dramatically after AS-ODN treatment. (H) Relative expression levels of Rgs19 are presented after the normalization using GAPDH. Scale bars: A, B, C, D, E, F, 500 μm; G, H, 100 μm.

3.3. *Knockdown of Rgs19 affects palatal fusion with cellular events*

Based on the specific expression pattern of *Rgs19*, which was observed mainly in the MEE, it was hypothesized that Rgs19 would play similar roles to Wnt11 during the process of MES removal (Fig. 1). Morphological examinations of the palatal fusion and cellular events including cell proliferation and apoptosis were examined after Rgs19 knockdown after 2 days cultivation at E13 (Figs. 3 and 4). This is because the one day cultivations at E13 were insufficient to examine the failure of palatal fusion with dramatic changes. The restricted areas of the palatal shelves were designated and examined to determine the precise roles of Rgs19 in palatal fusion. The middle part of the palate along with the upper molar forming regions showed the first attachment of both palatal shelves for fusion at E14 (Fig. 1J). After knocking down *Rgs19* with the AS-ODN treatment, the level of palatal fusion was examined carefully using computer-aided three dimensional reconstruction methods after serial frontal sections (Fig. 3). Immunostaining of pan-Cytokeratins, a marker for epithelial cells, was employed to observe the epithelial tissue remaining precisely after palatal fusion (Fig. 3A and B). AS-ODN for the *Rgs19*-treated specimens showed a much wider range of pan-Cytokeratin positive areas in the MES regions (Fig. 3B, D and F). Interestingly, much of the epithelial cells remaining were detected in the ventral side of the MES region (Fig. 3D and F). The area of pan-Cytokeratin positive tissues was measured after a 3D reconstruction using the "Image J" software to examine the objective levels of the epithelium remaining in the MES region (Fig. 3G). In addition, the Trowell's modified cultivations for 1 and 2 days at E13 was performed to examine the detailed procedures of palatal fusion after the treatments of AS-ODN for Rgs19 (Supplementary Figs. S1 and S2). These results were similar to those of roller cultivated explants (Figs. 2 and 3).

After 2 days cultivation at E13, the control specimens showed MES degradation, which was examined at E14.5 (Fig. 4A and C). Palatal epithelium in the MES regions of the control specimens showed a lower rate of proliferation than those of the AS-ODN-treated specimens (Fig. 4A and B). In particular, AS-ODN for the *Rgs19*-treated specimens showed the mesenchymal localization of Ki67 positive cells in the MES and underlying mesenchymal region (Fig. 4E). Compared to the control specimen, the ventral part of the palatal shelves showed Ki67 positive epithelial cells remaining in the MES region (Fig. 4B′, B″). In addition, the oral and nasal epithelium also showed stronger Ki67 positive cells than those of the AS-ODN treated specimen. The level of apoptosis was examined using a TUNEL assay (Fig. 4C and D). In the control specimens, massive apoptotic epithelial cells were detected in the dorsal part of MES (Fig. 4C). On the other hand, the number of apoptotic cells decreased after the AS-ODN treatment for Rgs19 (Fig. 4D and F). The sense-ODN and Scrambled-

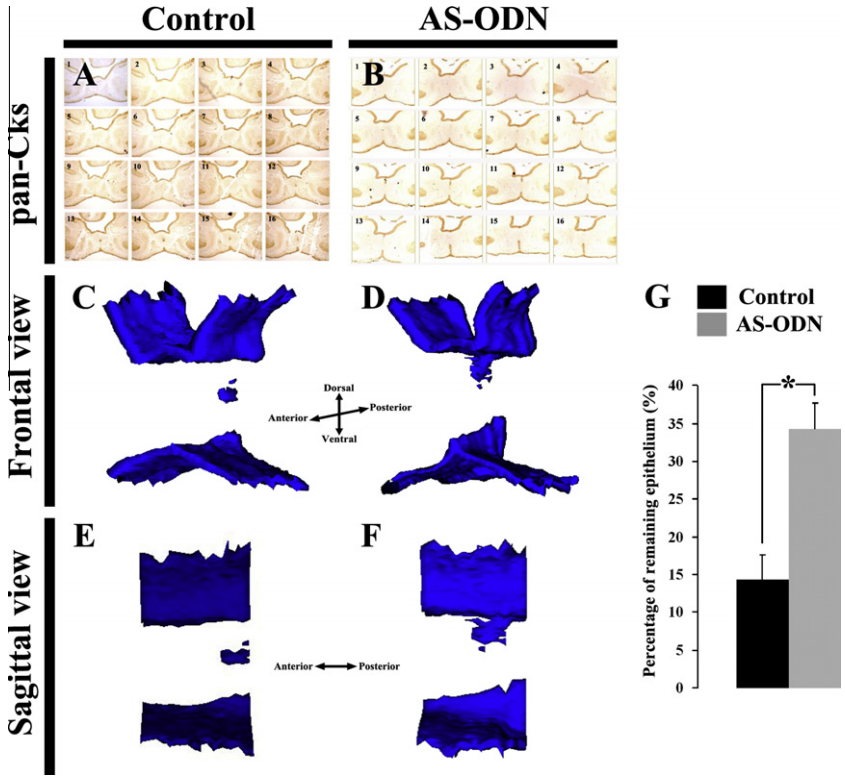

Fig. 3 – Three-dimensional reconstruction after the immunostaining against pan-Cytokeratins. After the 2 days cultivations at E13, middle parts of palatal fusion area along with the upper molar forming regions were reconstructed. (A and B) Serial frontal section views after the pan-Cytokeratins immunostainings from anterior to posterior direction. (C and D) Palatal epithelial tissues, which show the positive staining of pan-Cytokeratins, are reconstructed. (E and F) Sagittal views after the reconstructions. (G) Remaining epithelial tissues in the MES regions are examined using "Image J" software. $^{*}P < 0.05$ as determined by t-test.

ODN-treated specimens showed identical results to those of the control (data not shown). After Ki67 immunostaining and TUNEL assay, the number of positive cells in the designated region and MES region were measured (Fig. 4E and F). The results from knockdown of Rgs19 suggested that Rgs19 plays roles in palatal fusion through mechanisms including cell proliferation and apoptosis.

3.4. *Altered expression patterns of EMT related genes after the knockdown of Rgs19*

This study examined the altered expression patterns of well-known signaling molecules in palatogenesis using genome wide screening and RT-qPCR after knocking down Rgs19 at E13 followed by 1 day *in vitro* cultivation. To perform this experiment, culture explants showing unfused palatal shelves were collected and the MEE tissue was micro dissected carefully (Fig. 2I) because Rgs19 is expressed in the MEE not the MES (Fig. 1). At least 10 specimens were used for both the AS-ODN and control (S-ODN) treated groups. RNA samples were processed on Mouse gene 1.0 ST array (Affymetrix Inc.). From this pool of genes, 174 genes were shown with more than twofold regulated. 95 genes were identified as twofold up-regulated genes in the Rgs19 AS-ODN than the S-ODN. In contrast, 79 genes with twofold higher expression levels in the Rgs19 S-ODN compared to the AS-ODN were detected (Supplementary Tables S1 and S2). Supplementary Table S3 presents the gene numbers in the category classified according to molecular function. Supplementary Table S4 provides detailed gene lists with the microarray expression comparison data according to their molecular function group. In biological processes, the metabolism response related to cell adhesion, cell differentiation responses, and signal transduction were higher in Rgs19 AS-ODN, whereas the immune response gene, which mediates the complement activation and cellular defense responses, were lower in S-ODN. Genes, such as BMP2, EphB2/B3, Fgf10, Smad2 and Twist, were previously reported to be expressed strongly in palatal fusion. Initially, the expression patterns of Wnt responsive genes, which are reported to be crucial players in the palatal fusion process, were examined (Behrens et al., 1996; Jho et al., 2002; Tetsu and McCormick, 1999). The target genes of Wnt signaling including Axin2, Lef1 and CyclinD1 showed increased expression patterns after the *Rgs19* AS-ODN treatment (Fig. 5A). The palatal fusion related genes, such as Twist, Snail and Slug, showed lower expression patterns after the knockdown of *Rgs19* (Fig. 5A) (Martinez-Alvarez et al., 2004; Yu et al., 2008). The apoptosis-related molecules, including Caspase3, Bcl2, Caspase8, Bak1 and Fas, were evaluated to define the detailed function of *Rgs19* in the palatal fusion process via apoptosis. Interestingly, after the knockdown of Rgs19, Capase3, an apoptotic effecter,

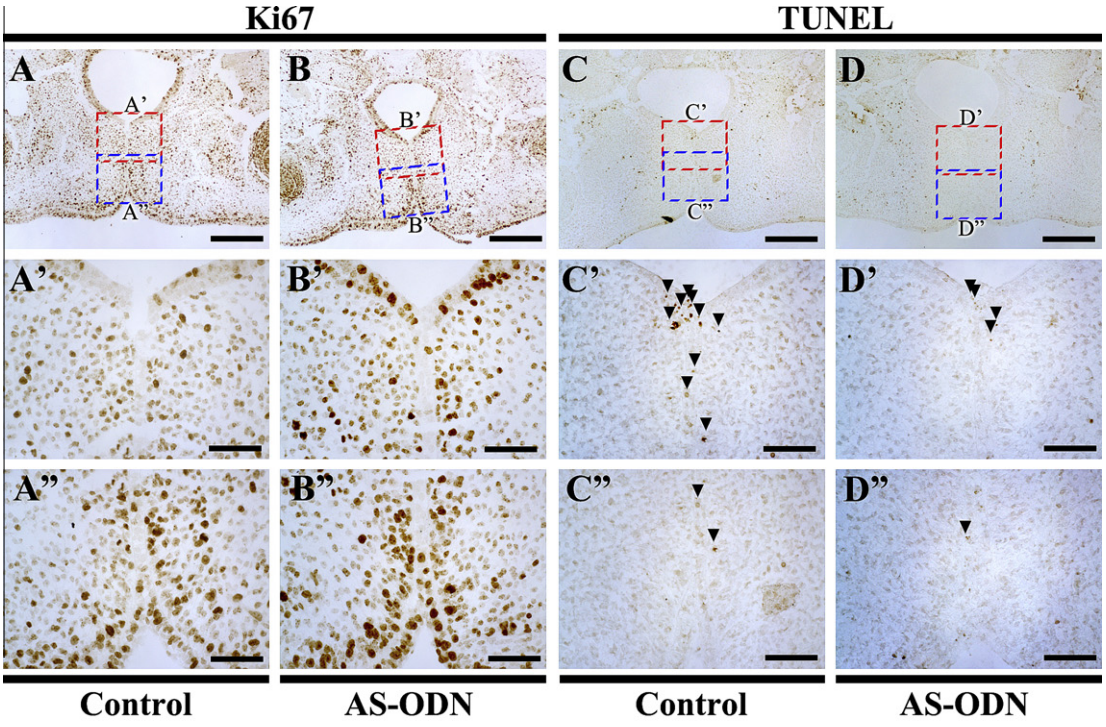

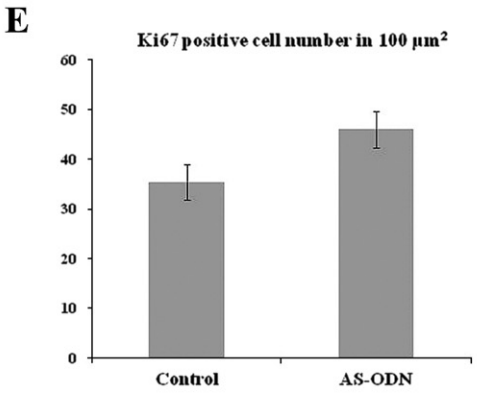

	Control (n=30)	AS-DON (n=30)
Numbers of Ki67 positive cells in 100 μm²	35.44	46.00
S.D.	±3.57	±3.67

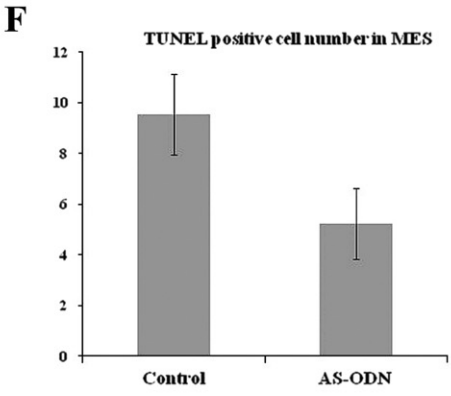

	Control (n=30)	AS-DON (n=30)
Numbers of TUNEL positive cells in MES	9.56	5.22
S.D.	±1.59	±1.39

Fig. 4 – Examinations of cellular events including cell proliferation and apoptosis after knocking down of Rgs19. (A and B) Ki67 immunostaining, (C and D) TUNEL assay on frontal sections after knockdown of Rgs19 after the 2 days cultivation at E13. (A and B) AS-ODN treated specimen shows increased localization pattern of Ki67 in the palatal fused area. (C and D) After the knocking down of Rgs19, TUNEL positive cells are much decreased in the palatal fused area. (E) Ki67 positive cells are counted in the 100 μm². (F) TUNEL positive cells were measured in the MES region. X′ and X″ are higher magnifications of X; scale bars: A–D, 200 μm; A′–D′, A″–D″, 50 μm.

showed an increased expression level. On the other hand, a significant decrease in the expression patterns of the other apoptosis-related molecules, including the anti-apoptotic factor, Bcl2, and the pro-apoptotic factors, Caspase8, Bak1 and Fas, was observed after the *Rgs19* AS-ODN treatment (Fig. 5A). Based on the expression patterns of the significant altered molecules, the precise expression pattern of *Tgfβ3*, which is a well known key signaling molecule for palatal fusion, in developing palatal shelves after 1 day cultivation at E13 was examined further. Compared to the control

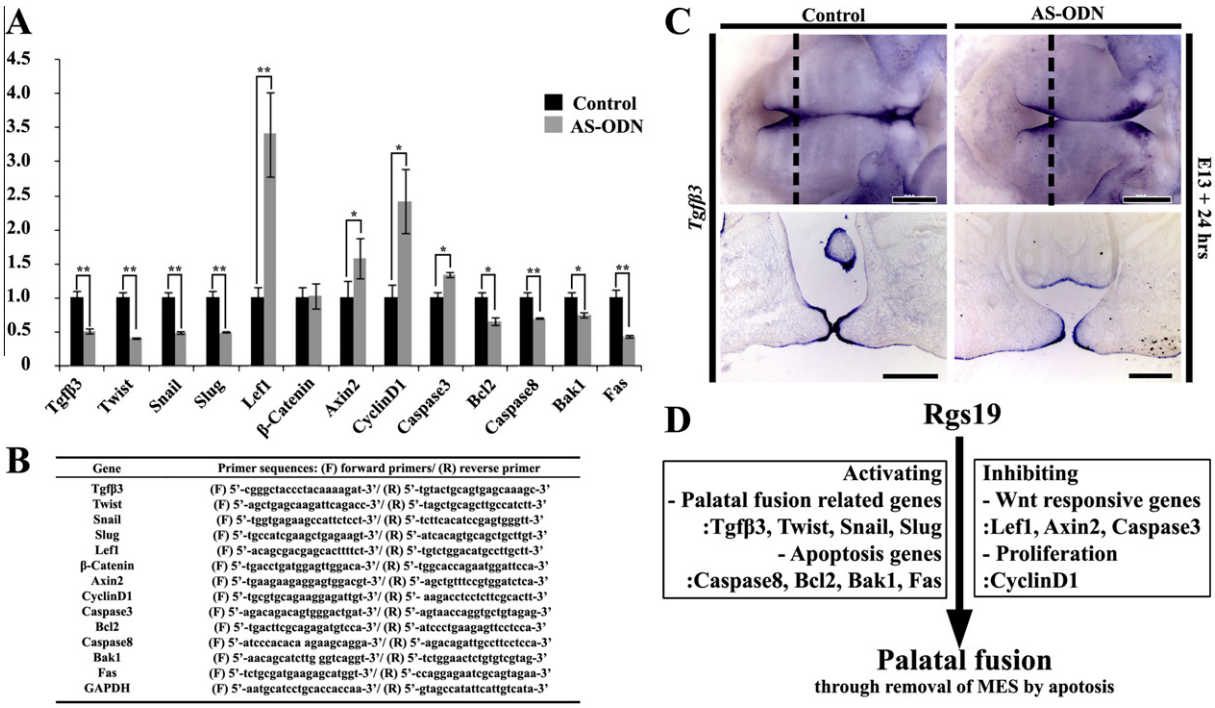

Gene	Primer sequences: (F) forward primers/ (R) reverse primer
Tgfβ3	(F) 5'-cgggctaccctacaaaagat-3'/ (R) 5'-tgtactgcagtgagcaaagc-3'
Twist	(F) 5'-agctgagcaagattcagacc-3'/ (R) 5'-tagctgcagcttgccatctt-3'
Snail	(F) 5'-tggtgagaagccattctcct-3'/ (R) 5'-tcttcacatccgagtgggtt-3'
Slug	(F) 5'-tgccatcgaagctgagaagt-3'/ (R) 5'-atcacagtgcagctgcttgt-3'
Lef1	(F) 5'-acagcgacgagcacttttct-3'/ (R) 5'-tgtctggacatgccttgctt-3'
β-Catenin	(F) 5'-tgacctgatggagttggaca-3'/ (R) 5'-tggcaccagaatggattcca-3'
Axin2	(F) 5'-tgaagaagaggagtggacgt-3'/ (R) 5'-agctgtttccgtggatctca-3'
CyclinD1	(F) 5'-tgcgtgcagaaggagattgt-3'/ (R) 5'- aagacctcctcttcgcactt-3'
Caspase3	(F) 5'-agacagacagtgggactgat-3'/ (R) 5'-agtaaccaggtgctgtagag-3'
Bcl2	(F) 5'-tgacttcgcagagatgtcca-3'/ (R) 5'-atcctgaagagttcctcca-3'
Caspase8	(F) 5'-atcccacaca agaagcagga-3'/ (R) 5'-agacagattgccttcctcca-3'
Bak1	(F) 5'-aacagcatcttg ggtcaggt-3'/ (R) 5'-tctggaactctgtgtcgtag-3'
Fas	(F) 5'-tctgcgatgaagagcatggt-3'/ (R) 5'-ccaggagaatcgcagtagaa-3'
GAPDH	(F) 5'-aatgcatcctgcaccaccaa-3'/ (R) 5'-gtagccatattcattgtcata-3'

Fig. 5 – Quantitative real time PCR and schematic diagram of putative roles of Rgs19 in palatal fusion. (A) Quantitative real time-PCR analysis detects altered expression patterns of candidate genes after the knocking down of Rgs19 for 1 day cultivation at E13. Expression levels of Lef1, Axin2, CyclinD1 and caspase3 are significantly up-regulated. Expression levels of Tgfβ3, Twist, Snail, Slug, Bcl2, caspase8, Bak1 and Fas are down-regulated. (B) Sequences of primers for RT-qPCR. (C) Whole mount *in situ* hybridization of Tgfβ3 and frontal frozen sections (scale bars for whole mount: 200 μm, for sections 100 μm). (D) Putative developmental function of Rgs19 in palatal fusion. $^{*}P < 0.05$ and $^{**}P < 0.01$ as determined by *t*-test.

cultivation, decreased *Tgfβ3* expression patterns were observed in the MEE regions of the palatal shelves after the Rgs19 AS-ODN treatment (Fig. 5C).

4. Discussion

This study examined the spatio-temporal expression patterns and developmental roles of Rgs19 in palate development. Based on the similar expression pattern of Rgs19 in developing mice palatal shelves to those of Wnt11 and Tgfβ3, which are important players in palatal fusion, it was hypothesized that Rgs19 is involved in palatal fusion. To define the detailed function of Rgs19 in palatogenesis, this study employed the *in vitro* organ culture method with AS-ODN treatments as a loss-of-function study at E13 for one and two days. After *in vitro* organ cultivations, the altered morphogenesis of the palatal shelves and expression patterns of related signaling molecules were examined using a range of experimental tools.

4.1. *Expression pattern and functional analysis of Rgs19 in mice palatogenesis*

The specific and restricted expression patterns of *Rgs19* were observed in the epithelial region of the palatal shelves from E12 to E14 (Fig. 1). Prior to palatal fusion, the expression pattern of Rgs19 was restricted more in the MEE region as palate develops (Fig. 1C, F and I). After palatal fusion, the epithelial expression of Rgs19 disappeared (Fig. 1L). On the other hand, the posterior palates where palatal fusion had not occurred showed a similar expression pattern to that observed at E13.5 (Fig. 1I and N). This specific expression pattern of epithelial Rgs19 coincided with those of Wnt11 and Tgfβ3, which are important signaling molecules in palatal development (Lee et al., 2008; Yang et al., 2008). These similar expression patterns suggest that Rgs19 plays similar or related roles in palatal development because the synexpression patterns of the signaling molecules would show similar or related functions in embryogenesis. A study of Tgfβ3 knock-out mice revealed a cleft palate through an alteration of apoptosis and fusion in palatogenesis (Taya et al., 1999). The knockdown of Wnt11, which showed a similar expression pattern to Rgs19 in the MEE region, was reported to alter the level of palatal shelf fusion by perturbing the apoptosis of the MES (Lee et al., 2008). The similar expression pattern of Rgs19 to Tgfβ3 and Wnt11 in the MEE region prompted an examination of the developmental function of Rgs19 in palatal fusion through an apoptotic process (Gurley et al., 2004).

In vitro organ cultivation methods including roller and Trowell's modified methods were employed to evaluate the developmental roles of Rgs19 in palatal development (Lee et al., 2008; Sohn et al., 2011). The *in vitro* cultivation systems mimicked the *in vivo* palatal development. The developmental stages were determined from the morphological changes. To evaluate the roles of Rgs19, the knockdown system was evaluated using an AS-ODN treatment for Rgs19. This is

because the experimental tool has advantages in transport of AS-ODN into the cells through a combination of fluid-phase (pinocytosis), adsorptive and receptor-mediated endocytosis (Akhtar et al., 2000). After the AS-ODN treatments, a decreased expression pattern of Rgs19 was observed in the 1 day cultivated specimens with a low rate of palatal fusion (Fig. 2J). After the AS-ODN treatments for Rgs19 at E12 for 2 and 3 days, most of the cultivated specimens exhibited defects in palatal development including palatal fusion (data not shown). Therefore, *in vitro* cultivations at E13 were performed for 1 or 2 days to determine the reason for the failure of palatal fusion with the incomplete removal of MES. The sense and scrambled ODNs showed similar results to the control specimens (data not shown). After 1 day cultivation, the palatal shelves were carefully dissected under a dissecting microscope and the palatal shelves were then collected and pooled for further examinations (Fig. 2I). The knockdown of Rgs19 using AS-ODN produced a dramatic decrease in its mRNA expression level (Fig. 2J). The morphological and cellular alterations were examined using these *in vitro* organ cultivation systems with AS-ODN treatments.

4.2. Regulation of cellular events through Rgs19 expression in palatal fusion

After 2 days cultivation at E13, the morphological alterations during palatal fusion were examined using a computer-aided three-dimensional reconstruction method (Fig. 3). At the beginning of palatal fusion, the middle parts of the palatal shelves contact each other initially, and palatal fusion processes along the anteroposterior axis (Lee et al., 2008). The morphological changes in these palatal fusion-initiating regions of the palatal shelves, which are adjacent to the upper molar forming regions, were reconstructed using a computer-aided method (Fig. 3). After the three-dimensional reconstructions, sagittal section views of the MES regions were prepared from the reconstructed figures, and the area of the pan-Cytokeratin positive epithelial regions remaining was measured using "image J" software (Fig. 3G). The higher percentage of epithelium remaining in the MES regions after Rgs19 knockdown would result in retardation and incomplete palatal fusion. The three-dimensional reconstructions suggested that palatal fusion would be initiated from the anterior to the posterior and from the dorsal to the ventral directions of the palatal shelves. These results confirm the previous report showing the anteroposterior direction of MEE cell migration patterns during palatal fusion (Jin and Ding, 2006). The AS-ODN for the Rgs19-treated specimens showed an almost two times higher epithelial percentage remaining than those of the control (Fig. 3G). In addition, the thickness of the palatal shelves was increased slightly after knocking down Rgs19. These morphological changes with the retardation of palatal fusion in the MES region and with thickened palatal shelves could be explained by cellular events, such as a decrease in apoptosis of MES and an increase in mesenchymal cell proliferation underlying MES (Fig. 4).

As predicted from the expression pattern of Rgs19, the knockdown of Rgs19 resulted in obvious alteration patterns in cell proliferation and apoptosis in the palatal shelves. A much larger number of Ki67 positive cells than those of the control were observed in the remaining epithelium and underlying mesenchyme of the MES region after the AS-ODN treatments (Fig. 4E). On the other hand, there was a significant decrease in the number of apoptotic cells after the treatment of AS-ODN with Rgs19 (Fig. 4F). This suggests that Rgs19 modulate the apoptosis and cell proliferation in palatal development. The knockdown of Rgs19 would inhibit apoptosis during the removal of MES, which are essential to morphogenesis in palatal fusion (Cuervo and Covarrubias, 2004; Fitchett and Hay, 1989; Nawshad and Hay, 2003; Shuler et al., 1991, 1992).

4.3. Signaling regulations in palatal development through modulation of Rgs19

Altered expression patterns of signaling molecules were examined using a genome wide screening method (Supplementary Table S1). The morphological examinations using the computer-aided three-dimensional reconstruction demonstrated that the knockdown of Rgs19 would result in the failure of palatal fusion with the inhibited removal of MES. Based on these results, the molecular signaling network underlying Rgs19 involved in palatal fusion was investigated by comparing the Rgs19 AS-ODN and S-ODN specimens. The gene array identified 174 genes with 2-fold alteration (Supplementary Table S2). Overall, of the genes the identified arrays were predicted to have potential, apoptosis, proliferation and Wnt responsive genes. The 95 up-regulated and 75 down-regulated genes identified in the Rgs19 AS-ODN-treated specimens were classified and analyzed according to their molecular functions. The largest increases occurred in the metabolism, signal transduction and cell differentiation, which contain the genes involved in palatal fusion and cell adhesion. As expected from previous reports on Rgs19, the changes in growth factors and cytokines have all been associated with the G protein signaling pathway (De Vries et al., 2000; Ji et al., 2010). RT-qPCR and *in situ* hybridization methods were used to confirm the altered expression patterns of the candidate genes from the microarray. Firstly, this study examined the palatal fusion related genes including Twist, Snail, and Slug using RT-qPCR (Fig. 5A). A significant decrease in the expression patterns of these palatal fusion related genes indicated that Rgs19 is a key regulator in the palatal fusion process by modulating the expression patterns of the palatal fusion related genes.

The altered expression patterns of the Wnt responsive genes including Lef1, β-Catenin, Axin2, and CyclinD1 were also examined. Interestingly, after the knockdown of Rgs19, the Wnt responsive genes were similar to those of the microarray with increased expression patterns but β-Catenin showed no differences. These increased expression patterns of the Wnt responsive genes indicate that Rgs19 modulates the Wnt responsive genes in mice palatogenesis in a negative manner. This can be explained by a previous report on the Rgs19 modulation of Wnt/β-Catenin signaling through inactivation of the Gαo subunit (Feigin and Malbon, 2007). Apoptosis is a major form of programmed cell death, which is a controlled process to remove damaged, unnecessary or used cells, to maintain homeostasis and the organization of

developing tissues (Montero and Hurle, 2010; Peter and Krammer, 2003). The apoptotic genes, such as Caspase3, Caspase8, Bcl2, Bak1 and Fas, were selected based on a previous report (Montero and Hurle, 2010). Genes related to the apoptotic signal transductions, such as Bak1, Bcl2, Capase8 and Fas, showed the decreased expression levels. On the other hand, Caspase3, an effecter caspase, showed an increased expression pattern. This suggests that apoptosis in the palatal EMT process via the modulation of *Rgs19* would result from the Caspase8-related pathway (Peter and Krammer, 2003). In addition, as reported previously regarding Caspase3 dependent apoptosis, Wnt canonical signaling regulates cell proliferation through CyclinD1 (Juraver-Geslin et al., 2011). Similar to this report, Rgs19 would modulate the Wnt canonical signaling responsive genes, including Axin2 and CyclinD1, to remove the MES during palatal fusion. In particular, altered expression patterns of Tgfβ3 after the knockdown of Rgs19 can well explain the phenotype of the inhibition of apoptosis in the MES, and suggest that Rgs19 functions through Tgfb3 (Fig. 5C). These results suggest that Rgs19 plays fundamental roles in the removal of MES through apoptosis and the signaling modulations of specific genes, including the Wnt responsive and palatal fusion related genes.

The knockdown of Rgs19 resulted in retardations and defects in palatal fusion through the apoptosis pathway. A previous report showed that Rgs19 inhibits Wnt/β-catenin signaling (Feigin and Malbon, 2007). Therefore, this study examined localization patterns of cellular events, the altered expression patterns of the candidate signaling molecules including palatal fusion related genes, Wnt responsive genes and apoptotic genes. This study revealed the precise functions of Rgs19 via cellular modulations controlled by the expression of specific genes in palatal fusion by cell proliferation and apoptosis. On the other hand, an *in vitro* study is not enough to discover the complex functions of Rgs19 in various forms of organogenesis. For a better understanding of Rgs19, genetic manipulated mice should be considered.

Acknowledgements

This study was supported by a Grant of the Korea Healthcare technology R&D Project, Ministry of Health & Welfare, Republic of Korea (A080131).

Appendix A. Supplementary data

Supplementary data associated with this article can be found, in the online version, at http://dx.doi.org/10.1016/j.mod.2012.07.004.

REFERENCES

Akhtar, S., Hughes, M.D., Khan, A., Bibby, M., Hussain, M., Nawaz, Q., Double, J., Sayyed, P., 2000. The delivery of antisense therapeutics. Adv. Drug Deliv. Rev. 44, 3–21.

Behrens, J., von Kries, J.P., Kuhl, M., Bruhn, L., Wedlich, D., Grosschedl, R., Birchmeier, W., 1996. Functional interaction of beta-catenin with the transcription factor LEF-1. Nature 382, 638–642.

Chiquet, B.T., Blanton, S.H., Burt, A., Ma, D., Stal, S., Mulliken, J.B., Hecht, J.T., 2008. Variation in WNT genes is associated with non-syndromic cleft lip with or without cleft palate. Hum. Mol. Genet. 17, 2212–2218.

Chou, M.J., Kosazuma, T., Takigawa, T., Yamada, S., Takahara, S., Shiota, K., 2004. Palatal shelf movement during palatogenesis: a fate map of the fetal mouse palate cultured in vitro. Anat. Embryol. (Berl.) 208, 19–25.

Cuervo, R., Covarrubias, L., 2004. Death is the major fate of medial edge epithelial cells and the cause of basal lamina degradation during palatogenesis. Development 131, 15–24.

De Vries, L., Mousli, M., Wurmser, A., Farquhar, M.G., 1995. GAIP, a protein that specifically interacts with the trimeric G protein G alpha i3, is a member of a protein family with a highly conserved core domain. Proc. Natl. Acad. Sci. U. S. A. 92, 11916–11920.

De Vries, L., Zheng, B., Fischer, T., Elenko, E., Farquhar, M.G., 2000. The regulator of G protein signaling family. Annu. Rev. Pharmacol. Toxicol. 40, 235–271.

Feigin, M.E., Malbon, C.C., 2007. RGS19 regulates Wnt-beta-catenin signaling through inactivation of Galpha(o). J. Cell Sci. 120, 3404–3414.

Fitchett, J.E., Hay, E.D., 1989. Medial edge epithelium transforms to mesenchyme after embryonic palatal shelves fuse. Dev. Biol. 131, 455–474.

Gritli-Linde, A., 2007. Molecular control of secondary palate development. Dev. Biol. 301, 309–326.

Gurley, J.M., Wamsley, M.S., Sandell, L.J., 2004. Alterations in apoptosis and epithelial-mesenchymal transformation in an *in vitro* cleft palate model. Plast. Reconstr. Surg. 113, 907–914.

He, F., Xiong, W., Yu, X., Espinoza-Lewis, R., Liu, C., Gu, S., Nishita, M., Suzuki, K., Yamada, G., Minami, Y., Chen, Y., 2008. Wnt5a regulates directional cell migration and cell proliferation via Ror2-mediated noncanonical pathway in mammalian palate development. Development 135, 3871–3879.

Hoffman, M.P., Kidder, B.L., Steinberg, Z.L., Lakhani, S., Ho, S., Kleinman, H.K., Larsen, M., 2002. Gene expression profiles of mouse submandibular gland development: FGFR1 regulates branching morphogenesis in vitro through BMP- and FGF-dependent mechanisms. Development 129, 5767–5778.

Hollinger, S., Hepler, J.R., 2002. Cellular regulation of RGS proteins: modulators and integrators of G protein signaling. Pharmacol. Rev. 54, 527–559.

Jho, E.H., Zhang, T., Domon, C., Joo, C.K., Freund, J.N., Costantini, F., 2002. Wnt/beta-catenin/Tcf signaling induces the transcription of Axin2, a negative regulator of the signaling pathway. Mol. Cell. Biol. 22, 1172–1183.

Ji, Y.R., Kim, M.O., Kim, S.H., Yu, D.H., Shin, M.J., Kim, H.J., Yuh, H.S., Bae, K.B., Kim, J.Y., Park, H.D., Lee, S.G., Hyun, B.H., Ryoo, Z.Y., 2010. Effects of regulator of G protein signaling 19 (RGS19) on heart development and function. J. Biol. Chem. 285, 28627–28634.

Jin, J.Z., Ding, J., 2006. Analysis of cell migration, transdifferentiation and apoptosis during mouse secondary palate fusion. Development 133, 3341–3347.

Juraver-Geslin, H.A., Ausseil, J.J., Wassef, M., Durand, B.C., 2011. Barhl2 limits growth of the diencephalic primordium through Caspase3 inhibition of beta-catenin activation. Proc. Natl. Acad. Sci. U. S. A. 108, 2288–2293.

Kang, P., Svoboda, K.K., 2002. PI-3 kinase activity is required for epithelial-mesenchymal transformation during palate fusion. Dev. Dyn. 225, 316–321.

Kemler, R., Hierholzer, A., Kanzler, B., Kuppig, S., Hansen, K., Taketo, M.M., De Vries, W.N., Knowles, B.B., Solter, D., 2004. Stabilization of beta-catenin in the mouse zygote leads to

premature epithelial-mesenchymal transition in the epiblast. Development 131, 5817–5824.
Kim, J.Y., Cho, S.W., Lee, M.J., Hwang, H.J., Lee, J.M., Lee, S.I., Muramatsu, T., Shimono, M., Jung, H.S., 2005. Inhibition of connexin 43 alters Shh and Bmp-2 expression patterns in embryonic mouse tongue. Cell Tissue Res. 320, 409–415.
Kim, J.Y., Lee, M.J., Cho, K.W., Lee, J.M., Kim, Y.J., Jung, H.I., Cho, J.Y., Cho, S.W., Jung, H.S., 2009. Shh and ROCK1 modulate the dynamic epithelial morphogenesis in circumvallate papilla development. Dev. Biol. 325, 273–280.
Lee, J.M., Kim, J.Y., Cho, K.W., Lee, M.J., Cho, S.W., Kwak, S., Cai, J., Jung, H.S., 2008. Wnt11/Fgfr1b cross-talk modulates the fate of cells in palate development. Dev. Biol. 314, 341–350.
Liu, W., Sun, X., Braut, A., Mishina, Y., Behringer, R.R., Mina, M., Martin, J.F., 2005. Distinct functions for Bmp signaling in lip and palate fusion in mice. Development 132, 1453–1461.
Logan, C.Y., Miller, J.R., Ferkowicz, M.J., McClay, D.R., 1999. Nuclear beta-catenin is required to specify vegetal cell fates in the sea urchin embryo. Development 126, 345–357.
Mailleux, A.A., Tefft, D., Ndiaye, D., Itoh, N., Thiery, J.P., Warburton, D., Bellusci, S., 2001. Evidence that SPROUTY2 functions as an inhibitor of mouse embryonic lung growth and morphogenesis. Mech. Dev. 102, 81–94.
Martinez-Alvarez, C., Blanco, M.J., Perez, R., Rabadan, M.A., Aparicio, M., Resel, E., Martinez, T., Nieto, M.A., 2004. Snail family members and cell survival in physiological and pathological cleft palates. Dev. Biol. 265, 207–218.
Martinez-Alvarez, C., Tudela, C., Perez-Miguelsanz, J., O'Kane, S., Puerta, J., Ferguson, M.W., 2000. Medial edge epithelial cell fate during palatal fusion. Dev. Biol. 220, 343–357.
Montero, J.A., Hurle, J.M., 2010. Sculpturing digit shape by cell death. Apoptosis Int. J. Prog. Cell Death 15, 365–375.
Nawshad, A., 2008. Palatal seam disintegration: to die or not to die? that is no longer the question. Dev. Dyn. 237, 2643–2656.
Nawshad, A., Hay, E.D., 2003. TGFbeta3 signaling activates transcription of the LEF1 gene to induce epithelial mesenchymal transformation during mouse palate development. J. Cell Biol. 163, 1291–1301.
Peter, M.E., Krammer, P.H., 2003. The CD95(APO-1/Fas) DISC and beyond. Cell Death Differ. 10, 26–35.
Ross, E.M., Wilkie, T.M., 2000. GTPase-activating proteins for heterotrimeric G proteins: regulators of G protein signaling (RGS) and RGS-like proteins. Annu. Rev. Biochem. 69, 795–827.
Shuler, C.F., Guo, Y., Majumder, A., Luo, R.Y., 1991. Molecular and morphologic changes during the epithelial-mesenchymal transformation of palatal shelf medial edge epithelium *in vitro*. Int. J. Dev. Biol. 35, 463–472.
Shuler, C.F., Halpern, D.E., Guo, Y., Sank, A.C., 1992. Medial edge epithelium fate traced by cell lineage analysis during epithelial-mesenchymal transformation *in vivo*. Dev. Biol. 154, 318–330.
Sohn, W.J., Yamamoto, H., Shin, H.I., Ryoo, Z.Y., Lee, S., Bae, Y.C., Jung, H.S., Kim, J.Y., 2011. Importance of region-specific epithelial rearrangements in mouse rugae development. Cell Tissue Res. 344, 271–277.
Taniguchi, K., Sato, N., Uchiyama, Y., 1995. Apoptosis and heterophagy of medial edge epithelial cells of the secondary palatine shelves during fusion. Arch. Histol. Cytol. 58, 191–203.
Taya, Y., O'Kane, S., Ferguson, M.W., 1999. Pathogenesis of cleft palate in TGF-beta3 knockout mice. Development 126, 3869–3879.
Tetsu, O., McCormick, F., 1999. Beta-catenin regulates expression of cyclin D1 in colon carcinoma cells. Nature 398, 422–426.
Warner, D.R., Smith, H.S., Webb, C.L., Greene, R.M., Pisano, M.M., 2009. Expression of Wnts in the developing murine secondary palate. Int. J. Dev. Biol. 53, 1105–1112.
Yang, L.T., Li, W.Y., Kaartinen, V., 2008. Tissue-specific expression of Cre recombinase from the Tgfb3 locus. Genesis 46, 112–118.
Yu, W., Kamara, H., Svoboda, K.K., 2008. The role of twist during palate development. Dev. Dyn. 237, 2716–2725.
Yu, W., Serrano, M., Miguel, S.S., Ruest, L.B., Svoboda, K.K., 2009. Cleft lip and palate genetics and application in early embryological development. Indian J. Plast. Surg. 42 (Suppl), S35–50.